TÜBİTAK

Turk J Elec Eng & Comp Sci, Vol.20, No.1, 2012, © TÜBİTAK
doi:10.3906/elk-1001-397

Tunable SRR-based substrate for a microstrip patch antenna

Adnan SONDAŞ*, Mustafa Hikmet Bilgehan UÇAR, Yunus Emre ERDEMLİ
Department of Electronics and Computer Education, Kocaeli University,
41380 Kocaeli-TURKEY
e-mails: {asondas, mhbucar, yunusee}@kocaeli.edu.tr

Received: 29.01.2010

Abstract

In this paper, a microstrip patch antenna over an artificial substrate composed of split-ring resonator (SRR) elements is introduced. As the SRR-based substrate provides miniaturization for the patch, metallic loadings placed between the rings of the SRR elements offer frequency-tuning capability. Practical switch models are employed in lieu of those loadings to demonstrate dynamic control of the operational frequency. The full-wave analysis and design of the proposed tunable patch were carried out using CST Microwave Studio, and the cross-comparisons were provided via Ansoft HFSS. Preliminary measurements are also presented, demonstrating the prospective performance of the proposed design.

Key Words: *Microstrip patch antenna, split-ring resonator, frequency tuning, miniaturization, practical switch modeling*

1. Introduction

Multifunctionality plays a major role in today's communication systems, where size, weight, and cost are the main limiting factors in designing integrated transceiver circuitry. In this context, electronically reconfigurable printed antennas were previously considered in polarization-diverse or multiband applications [1-5]. In those studies, an antenna element itself was reconfigured via appropriate switching. Alternatively, one can tailor the frequency response of the substrate to achieve enhanced antenna operation [6]. The goal of this study was to offer a new concept of frequency-tunable substrate for a microstrip antenna to achieve multifrequency operation.

Split-ring resonator (SRR) elements with inherent μ-negative behavior [7] have been used as building blocks of metamaterial structures in various filter applications for over a decade [8,9]. There have been several studies on tunable SRR filters [10-12], in which the varactor switches or capacitive loads placed between the SRR splits or the ring elements have mainly controlled the frequency-tuning performance. We also proposed such tunable SRR filters in [13-15]. However, the use of SRR elements in antenna applications is a rather new topic. Recently, split-ring microstrip antennas were proposed for dual-band WLAN applications [16,17].

*Corresponding author: Department of Electronics and Computer Education, Kocaeli University, 41380 Kocaeli - TURKEY

SRR elements were also utilized as composite substrates providing miniaturization for patch antennas [18-20]. There was no frequency-tuning capability reported in those antenna studies. In this research, we propose a new switching configuration to dynamically control the frequency behavior of the SRR substrate placed underneath a patch antenna. To the best of our knowledge, the proposed configuration presented in this study is the first utilization of tunable SRR elements in an antenna application.

We propose an artificial substrate composed of SRR elements providing frequency tuning as well as miniaturization for a microstrip patch antenna. The frequency tuning is achieved by means of several metallic loadings placed appropriately between the rings of each SRR element. Similar loading configurations were previously employed in recent SRR filter structures [13-15]. In practice, those loadings may be replaced by on/off switches for dynamic frequency tuning. In this paper, we also consider practical switch modeling in the SRR-based substrate to demonstrate possible switch effects on the patch performance. Furthermore, preliminary measurement results for the proposed SRR substrate with metallic loadings are presented, demonstrating promising tunable patch operation.

The full-wave analysis of the proposed antenna design was carried out using CST Microwave Studio based on the time-domain finite-integration technique. The cross-comparisons were provided by using Ansoft HFSS, which utilizes the frequency-domain finite-element method.

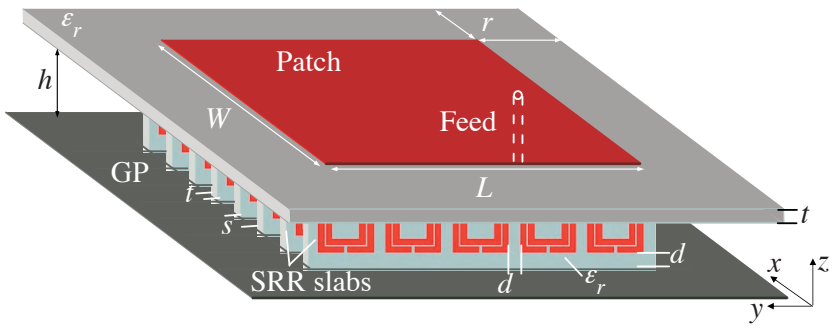

Figure 1. Proposed MPA/SRR configuration: $L = W = 21$, $r = 5$, $h = 4.5$, $t = 0.5, s = 3$, $d = 1$, all in mm; $\varepsilon_r = 2.2$.

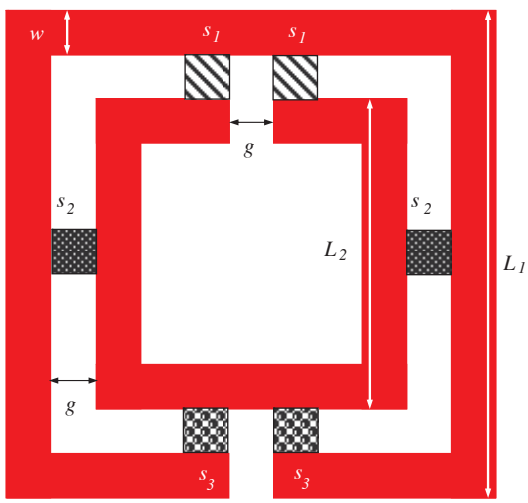

Figure 2. Proposed tunable SRR configuration: $L_1 = 3.5$, $L_2 = 2.5$, $w = g = 0.25$, all in mm.

2. Numerical design

We now introduce the microstrip patch antenna (MPA) design over the frequency-tunable SRR-based substrate. The proposed MPA/SRR configuration is depicted in Figure 1. As shown, the MPA excited by a 50-Ω coaxial feed is placed over a composite substrate consisting of 8 SRR slabs, all backed by the ground plane (GP). Each SRR slab contains 5 SRR elements supported by a thin substrate (Rogers RT/duroid 5880, $t = 0.5$ mm, $\varepsilon_r = 2.2$), and each SRR element includes 3 pairs of metallic loadings or pads (s_1, s_2, s_3) appropriately inserted between the rings (Figure 2) for frequency-tuning purposes. To achieve the desired antenna performance, the SRR splits as well as the SRR slabs are placed along the same direction with the E-field excited on the antenna element.

The full-wave analysis and design of the tunable MPA/SRR structure were carried out using CST Microwave Studio, and the cross-comparisons were provided by means of Ansoft HFSS. We carried out a number of parametric studies to achieve the optimum design parameters. The optimization was processed using the automatic optimization tools available in the simulators. The critical parameters considered in that process were SRR dimensions, the placement of SRR elements with respect to the patch, the locations of the metallic loads (switch location in a practical realization), the placement of the feed, and the patch dimensions.

The return loss characteristics of the MPA/SRR designs via 2 different simulators are displayed in Figure 3. As seen, the simulation results are in quite good agreement. While the MPA in the absence of the SRR slabs (that is, the MPA backed by the substrate with a thickness of $t = 0.5$ mm is placed over an air-filled cavity at a distance of $h = 4.5$ mm above the GP) has a resonance around 5.65 GHz, the inclusion of the SRR substrate without loadings results in the reduced resonance frequency of 4.35 GHz and thus miniaturization with a ratio of 1.3. More importantly, when each pair of loadings (s_1, s_2, s_3) is individually placed in the corresponding locations, the resonance shifts upwards to a respective frequency as compared to the no-loading case, as seen in Figure 3. In particular, the loadings placed equidistant from each of the splits (s_2) provide an operation around 4.75 GHz, whereas the loadings closer to the split of the outer ring (s_3) and the loadings closer to the split of the inner ring (s_1) allow for operation at a higher band (around 4.85 GHz) and at a lower band (around 4.6 GHz), respectively. Hence, the tunable MPA/SRR design offers a frequency-tuning operation over a band of 4.3-4.9 GHz with almost 7% bandwidth ($S_{11} < -10$ dB with a 50-Ω system impedance) for all cases considered. In addition, by varying the locations of the loadings around the loop between the rings, the corresponding resonant frequencies may be adjusted to desired frequencies within the band of interest. Also note that, when more than one pair of metallic pads is present in the SRR elements at the same time, the patch does not resonate in the corresponding band.

The pattern/gain characteristics are almost not altered due to the loaded SRR substrate, and thus all of the designs considered result in similar radiation characteristics. As a representative radiation performance, the broadside radiation patterns (2D and 3D) at 4.85 GHz are displayed for the MPA/SRR configuration with s_3 loadings in Figure 4. As can also be seen in the Table, the MPA/SRR designs offer a directivity of about 8 dBi, which is almost 1 dB less than that of the MPA in the absence of the SRR slabs. This small reduction in the directivity due to the loading effect of the SRR is not critical since the directivity performance is not a priority of the proposed design. We also note that the computed radiation efficiencies for all of the MPA designs presented here are better than 98%.

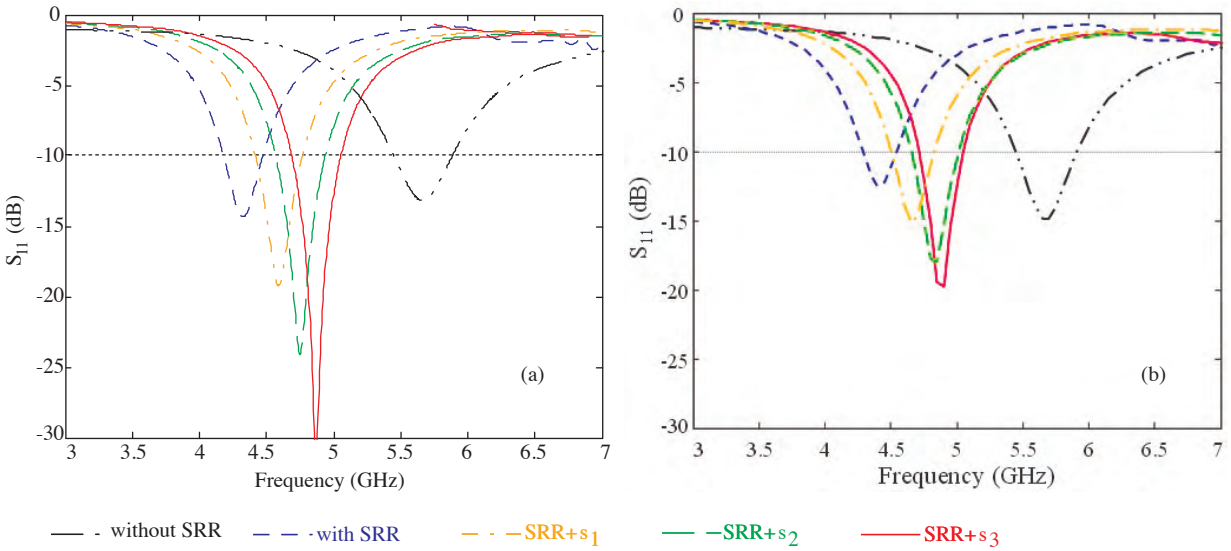

Figure 3. Return loss characteristics of the MPA/SRR design via a) CST and b) HFSS.

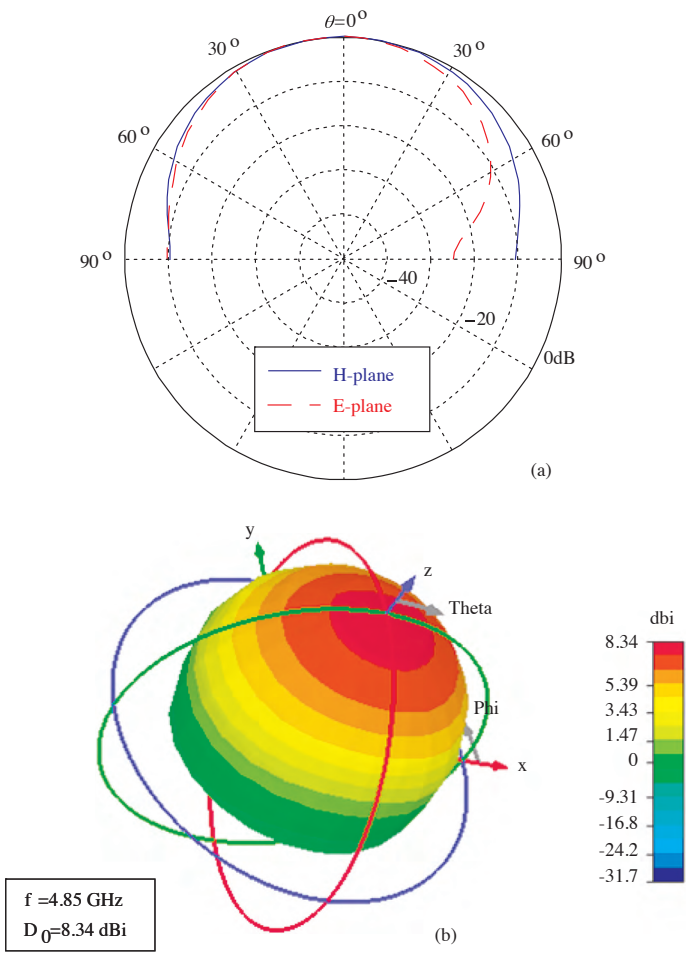

Figure 4. Radiation patterns of the MPA/SRR design with s_3 loadings for $f = 4.85$ GHz, a) 2D and b) 3D.

Table. Directive gain performance of the MPA/SRR designs.

Directivity	MPA/SRR designs				
	Without SRR, 5.65 GHz	With SRR, 4.35 GHz	SRR+s_1, 4.6 GHz	SRR+s_2, 4.75 GHz	SRR+s_3, 4.85 GHz
D_0 (dBi)	8.7	7.75	8.05	8.2	8.34

In practice, low-loss and high-isolation surface-mounted on/off switches (MEMS switches, PIN diodes, etc.) may be employed in lieu of those metallic loadings for dynamic control of the operational frequency. To demonstrate possible effects of the practical switches on MPA/SRR performance, we modeled the loadings as 2-legged bridges based on cantilever MEMS switch structure [21], as depicted in Figure 5. As seen, this simplistic model consists of a copper strip placed on 2 copper legs when the particular switch (s_2) is in the on-state. For the off-state, the copper strip is placed on only one copper leg (s_1 and s_3), while a possible capacitive effect is expected. A representative return loss (S_{11}) performance of the MPA/SRR design with the MEMS switch model is also shown in Figure 5. As seen, by the inclusion of the switch model, the frequency response is shifted downwards slightly (approximately 0.1 GHz) as compared to the response of the metallic-pad modeling (see Figure 3).

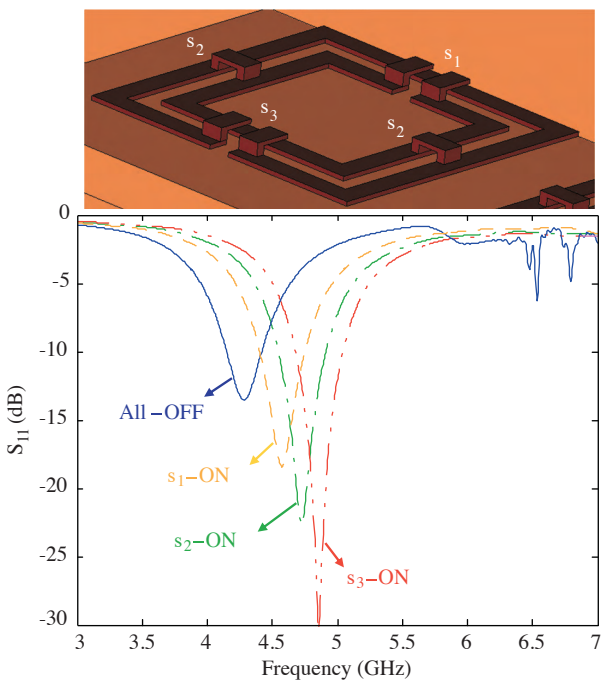

Figure 5. Frequency-tuning performance of the MPA/SRR design with bridge MEMS modeling. The switch positions s_2-ON and s_1 / s_3-OFF are depicted.

In the analysis, we also considered electrical equivalent models for practical PIN diodes in place of the metallic loadings. We modeled the loadings as capacitors (C = 0.3-1 pF) and resistors (R = 1–5 Ω) when they were in the off-state and the on-state, respectively, as depicted in Figure 6. Those capacitor and resistor values represent actual switch behavior in an approximate manner. The PIN-diode as well as MEMS switches would have inductive effects on the frequency response. However, in the analysis, we mainly focused on the capacitive

effect, which is considered to be the predominant one. A similar yet smaller effect on the tuning performance is expected with the inclusion of the inductive loading.

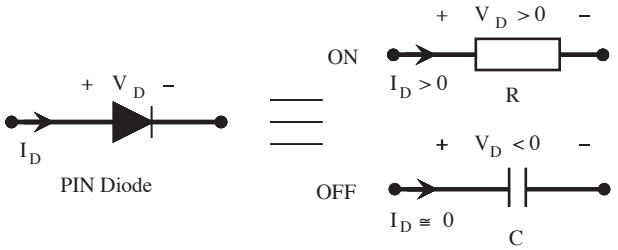

Figure 6. Simple circuit modeling of the PIN diode switch used in the analysis.

The S_{11} performances of the PIN diode and the MEMS switch models are shown in Figure 7 for comparison purposes. As seen, by the inclusion of the PIN model, the frequency response was shifted by 0.3 GHz on average as compared to the response of the bridge modeling. There was almost 5 dB of difference,

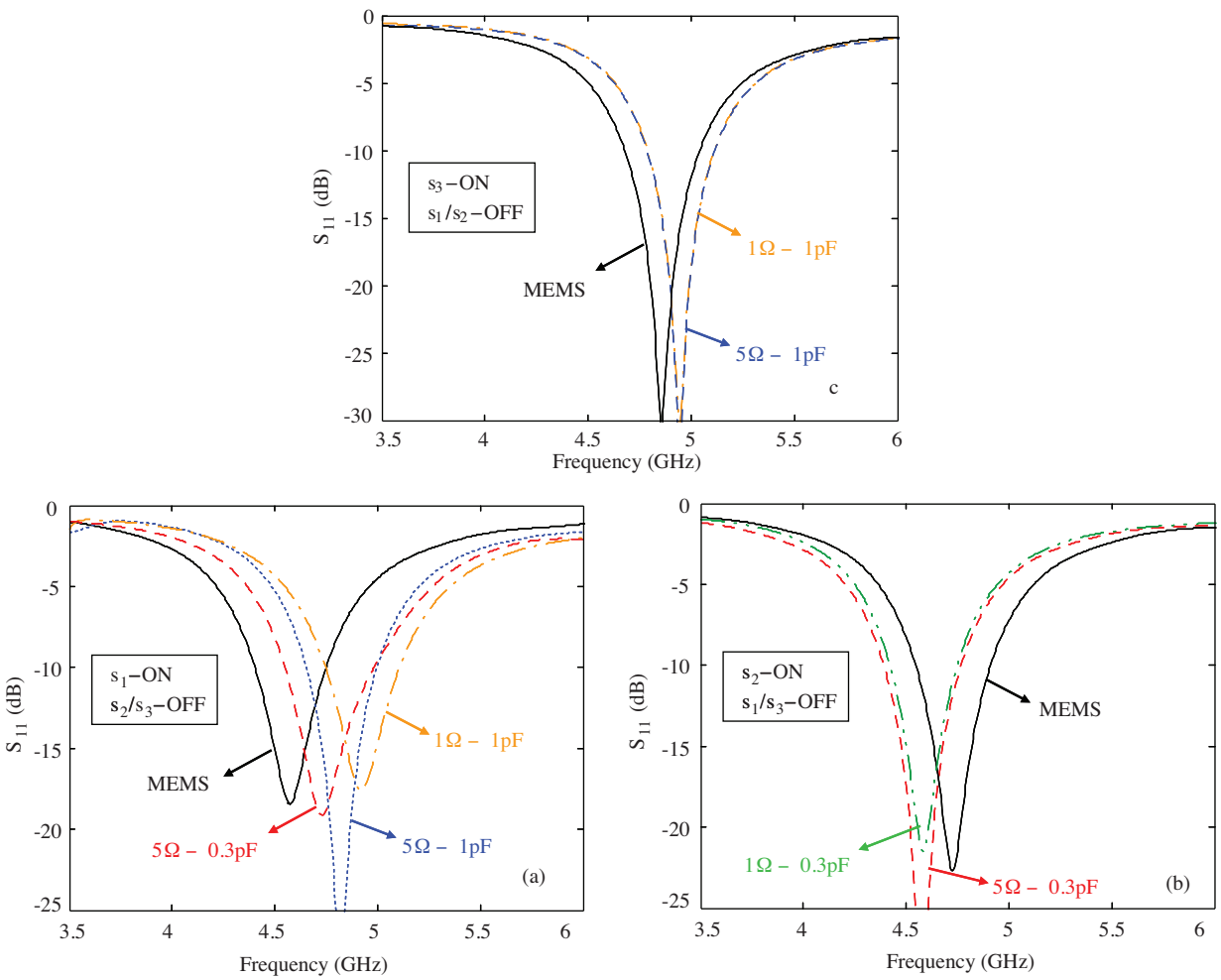

Figure 7. Return loss characteristics of the MPA/SRR design for MEMS (bridge) and PIN diode (circuit) models: a) s_1-ON and s_2/s_3-OFF, b) s_2-ON and s_1/s_3-OFF, c) s_3-ON and s_1/s_2-OFF.

on average, in the corresponding S_{11} levels. These variations due to tolerable switch effects are to be expected. The MPA/SRR design parameters in the presence of practical switch models can be reoptimized to achieve the performance in the desired frequencies. More importantly, the results promise frequency-tuning performance of the proposed MPA/SRR design in a practical implementation.

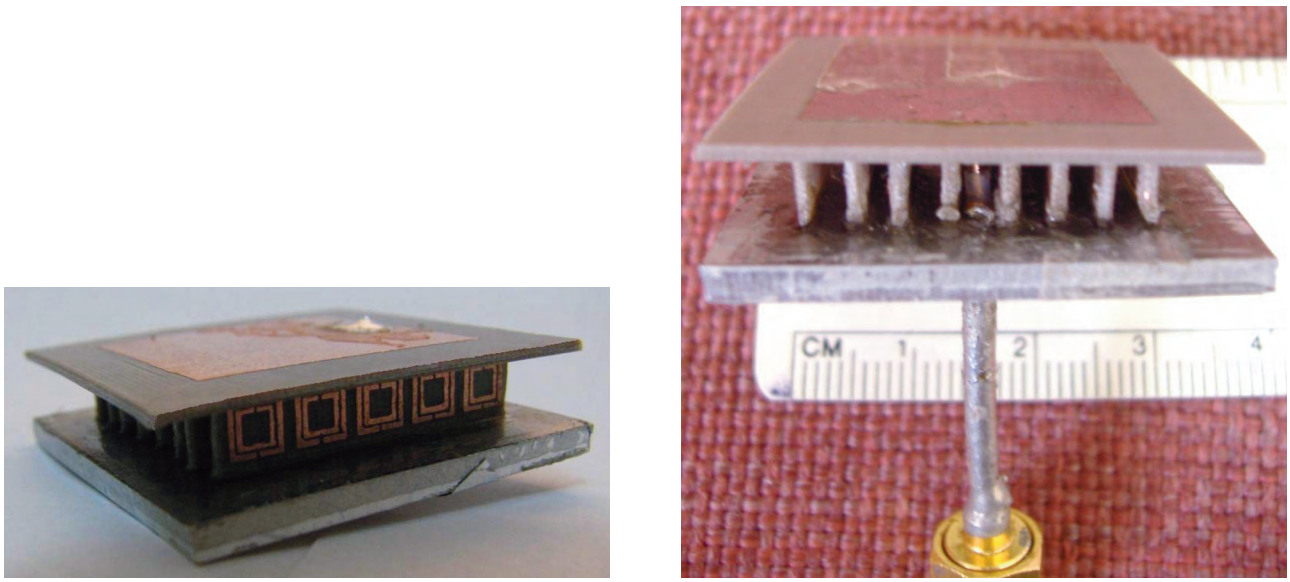

Figure 8. Fabricated MPA/SRR (no loading) prototype, of which 2 perspective views are shown.

3. Measurements

In order to validate the proposed tunable SRR-based substrate, 3 prototypes for the MPA/SRR designs were fabricated and return loss measurements were carried out. One of the prototypes consisted of the MPA in the

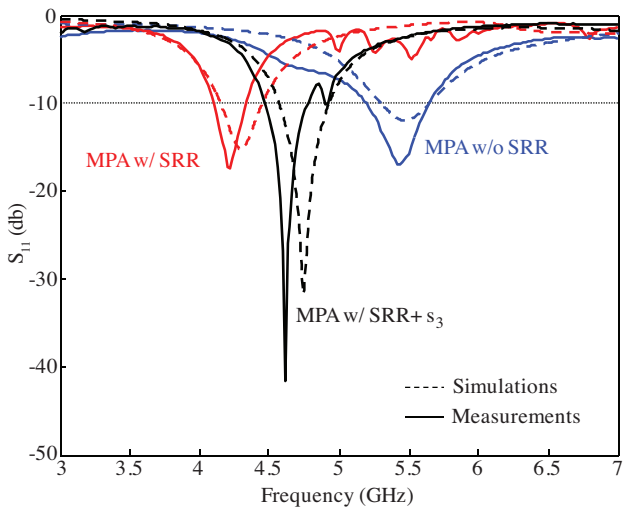

Figure 9. Simulated versus measured return loss characteristics of the MPA/SRR designs. The results for 3 cases are displayed, namely MPA in the absence of the SRR, MPA in the presence of the SRR (no loading), and MPA in the presence of SRR+s_3 loading (metallic pad).

absence of SRR slabs, while the others included the SRR slabs with and without metallic pads, where only the s_3 loading case was considered for a representative switching configuration (see Figure 2). A photograph of the MPA/SRR prototype is shown in Figure 8. At the time of fabrication, the substrate available to us was Arlon DiClad 880 with $t = 0.79$ mm and $\varepsilon_r = 2.2$. The thickness for this substrate differs from that used previously in simulations where the substrate thickness of 0.5 mm was employed. This difference would only cause a slight downward frequency shift in the S_{11} response. However, the tunable frequency response is still observed, as shown in Figure 9, where the simulated (remodeling with $t = 0.79$ mm) and measured return loss characteristics for the 3 prototypes are displayed. As shown, the measured and simulated data are in quite good agreement, with only a slight frequency shift (less than 3% considering the corresponding center frequencies). The prototypes also result in much better S_{11} levels as compared to their simulated counterparts, noting that those discrepancies are expected due to material and fabrication tolerances. More importantly, the frequency-tuning performance of the proposed SRR substrate is thus demonstrated with this preliminary realization.

4. Conclusion

In this paper, we introduced a microstrip patch antenna over a novel SRR-based substrate. It was numerically demonstrated that the composite substrate allows for miniaturization and frequency-tuning operation for the patch. The latter was accomplished by means of metallic loadings placed between the rings of the SRR elements. One can employ practical on/off switches in lieu of those metallic loadings to achieve multifrequency operation for the patch. For this purpose, simple equivalent models were employed in the SRR substrate to demonstrate the dynamic tuning performance of the proposed switching configuration. In addition, a preliminary practical realization of the proposed MPA/SRR design was carried out, providing reasonably good performance in accordance with the simulations.

We have demonstrated a new concept of tunable SRR substrate in this paper. For this, we chose a representative frequency band for the demonstration of the proposed idea, and there is no specific preference on that choice. One can easily change (scale) the design parameters to achieve a special design for a realistic frequency operation. In addition, the practical implementation of the proposed design requires the integration of low-loss and high-isolation surface-mounted switches (MEMS or PIN diodes) on the same SRR substrate. It is important to point out that the switches projected to be utilized in the design will be passive; that is, they will be on/off switches controlled by DC biasing, and there will be no radio-frequency signaling through the switch elements. It is expected that there may be unwanted parasitic effects of the bias circuitry on the performance, but they can be assessed and minimized in the implementation phase.

Acknowledgement

This work was supported by the Scientific and Technological Research Council of Turkey (TÜBİTAK) under Project No. 107E198. We would like to thank the anonymous reviewers for their invaluable comments.

References

[1] Y. Fan, Y. Rahmat-Samii, "A reconfigurable patch antenna using switchable slots for circular polarization diversity", Microwave Wireless Components Letters, Vol. 12, pp. 96-98, 2002.

[2] Y.E. Erdemli, R.A. Gilbert, J.L. Volakis, "A reconfigurable slot aperture design over a broadband substrate/feed structure", IEEE Transactions on Antennas and Propagation, Vol. 52, pp. 2860-2870, 2004.

[3] C.G. Christodoulou, D. Anagnostou, V. Zachou, "Reconfigurable multifunctional antennas", IEEE International Workshop on Antenna Technology - Small Antennas and Novel Metamaterials, pp. 176-179, 2006.

[4] B.A. Cetiner, G.R. Crusats, L. Jofre, N. Bıyıklı, "RF MEMS integrated frequency reconfigurable annular slot antenna", IEEE Transactions on Antennas and Propagation, Vol. 58, pp. 626-632, 2010.

[5] N. Behdad, K. Sarabandi, "Dual-band reconfigurable antenna with a very wide tunability range", IEEE Transactions on Antennas and Propagation, Vol. 54, pp. 409-416, 2006.

[6] Y.E. Erdemli, K. Sertel, R.A. Gilbert, D.E. Wright, J.L. Volakis, "Frequency selective surfaces to enhance performance of broad-band reconfigurable arrays", IEEE Transactions on Antennas and Propagation, Vol. 50, pp. 1716-1724, 2002.

[7] J.B. Pendry, A.J. Holden, D.J. Robins, W.J. Stewart, "Magnetism from conductors and enhanced nonlinear phenomena", IEEE Transactions on Microwave Theory and Techniques, Vol. 47, pp. 2075-2084, 1999.

[8] J. Kim, C.S. Cho, J.W. Lee, "CPW bandstop filter using slot-type SRRs", Electronics Letters, Vol. 41, pp. 1333-1334, 2005.

[9] I. Gil, J. Bonache, J. Garcia-Garcia, F. Falcone, F. Martin, "Metamaterials in microstrip technology for filter applications", Proceedings of Antennas and Propagation Society International Symposium, pp. 668-671, 2005.

[10] I. Gil, J. Garcia-Garcia, J. Bonache, F. Martin, M. Sorolla, R. Marques, "Varactor-loaded split ring resonators for tunable notch filters at microwave frequencies", Electronics Letters, Vol. 40, pp. 1347-1348, 2004.

[11] P. Sang-June, L. Kok-Yan, G.M. Rebeiz, "Low-loss 5.15-5.70-GHz RF MEMS switchable filter for wireless LAN applications", IEEE Transactions on Microwave Theory and Techniques, Vol. 54, pp. 3931-3939, 2006.

[12] K. Aydin, E. Ozbay, "Capacitor-loaded split ring resonators as tunable metamaterial components", Journal of Applied Physics, Vol. 101, doi: 10.1063/1.2427110, 2007.

[13] Y.E. Erdemli, A. Sondas, "Dual-polarized frequency-tunable composite left-handed slab", Journal of Electromagnetic Waves and Applications, Vol. 19, pp. 1907-1918, 2005.

[14] C. Cenk, A. Sondas, Y.E. Erdemli, "Tunable split ring resonator microstrip filter design", Proceedings of Mediterranean Microwave Symposium, pp. 20-23, 2006.

[15] M.H.B. Ucar, A. Sondas, Y.E. Erdemli, "Switchable split-ring frequency selective surfaces", PIERB, Vol. 6, pp. 65-79, 2008.

[16] S.C. Başaran, Y.E. Erdemli, "Dual-band split-ring antenna design for WLAN applications", Turkish Journal of Electrical Engineering and Computer Sciences, Vol. 16, pp. 79-86, 2008.

[17] S.C. Basaran, Y.E. Erdemli, "A dual-band split-ring monopole antenna for WLAN applications", Microwave and Optical Technology Letters, Vol. 51, pp. 2685-2688, 2009.

[18] M.K. Karkkainen, M. Ermutlu, S. Maslovski, P. Ikonen, S. Tretyakov, "Numerical simulations of patch antennas with stacked split-ring resonators as artificial magnetic substrates", IEEE International Workshop on Antenna Technology, pp. 395-398, 2005.

[19] M. Ermutlu, C.R. Simovski, M.K. Karkkainen, P. Ikonen, S.A. Tretyakov, A.A. Sochava, "Miniaturization of patch antennas with new artificial magnetic layers", IEEE International Workshop on Antenna Technology, pp. 87-90, 2005.

[20] M.F. Wu, F.Y. Meng, Q. Wu, J. Wu, L.W. Li, "Miniaturization of a patch antenna with dispersive double negative medium substrates", Proceedings of APMC, Vol. 1, doi: 10.1109/APMC.2005.1606177, 2005.

[21] G.M. Rebeiz, J.B. Muldavin, "RF-MEMS switches and switch circuits", IEEE Microwave Magazine, Vol. 2, pp. 59-71, 2001.